Proceedings of ICRC 2001: 42 © Copernicus Gesellschaft 2001

ICRC 2001

The SPHINX code for simulation of processes in X-ray emulsion chambers

R. Mukhamedshin

Institute for Nuclear Research, pr. 60-letiya Oktyabrya 7a, Moscow, 117312 Russia

Abstract. A three-dimensional Monte Carlo program is elaborated for simulations of processes in X-ray emulsion chambers and measurement procedures used in experiments both aboard stratospheric balloons and at mountain altitudes. The code is applicable from ~ 1 GeV to extremely high energies (~ 10 PeV) for arbitrary type of chamber design including lead, carbon, rubber, air, e.g. The code is easy in use and of access for all the persons via Internet.

1 Introduction

From the earliest days of performing the balloon-born and mountain-level X-ray emulsion chamber (EC) experiments, it was necessary to simulate physical processes in ECs as well as measurement procedures. Although a number of corresponding codes was elaborated and applied ((Dunaevsky and Zimin, 1988; Haungs *et al*., 2001; Galkin *et al*., 2000; Okamoto and Shibata, 1987), e.g.), only authors can really use these programs, and there is no a specialized free-access program which could be easily got and used by any person, like the *CORSIKA* code, whereas many scientists need to apply such a program to estimate possible ways of experiment improvement or solve current experimental problems.

This work describes the algorithm *SPHINX* (Simulation of Processes of Hadron and lepton INteractions in X-ray emulsion chamber) which is elaborated to change this situation. The executable file, setup program, and manual can be easily taken via Internet at

http://www.lebedev.ru/pages/pamir/sphinx.htm and

http://runjob.boom.ru/sphinx.htm.

The algorithm uses the MC0 code for simulation of hadron - nucleus and nucleus - nucleus interactions (Fedorova and Mukhamedshin, 1994).

Correspondence to: R.Mukhamedshin
(muhamed@sci.lebedev.ru)

2 Primary and secondary particles

At present, electrons and positrons, γ-rays, protons and He, Li, C,O,Mg,Si,V,Fe nuclei can be considered as primary particles arriving at the top of the chamber. The next version of the *SPHINX* will make possible to simulate all the particles listed in Table 1 as primary particles.

3 Particles

Table 1 lists types and codes of stable and semistable particles used in simulation and recording by the *SPHINX*. The mean free path for decay is taken into account for all the particles with life time $\tau_0 > 10^{-19}$ s.

Particle	Code	Particle	Code	Particle	Code
p	1	D^+	16	**V**	42
$\overline{p}$	2	D^-	17	**Fe**	43
n	3	$\overline{D}^0$	18	**Pb**	44
$\overline{n}$	4	D^0	19	$\overline{\Sigma}^-$	51
Λ^0	5	D_s^+	20	$\overline{\Sigma}^+$	52
$\overline{\Lambda}^0$	6	D_s^-	21	$\overline{\Sigma}^0$	52
Λ_c^+	7	Σ^+	33	e^+	63
Λ_c^-	8	Σ^-	34	e^-	64
π^+	9	Σ^0	35	γ	69
π^-	10	**He**	36	Ω^-	71
π^0	11	**Li**	37	Ω^+	72
K^+	12	**C**	38	ν	70
K^-	13	**O**	39	Ξ^0	181
K_S^0	14	**Mg**	40	Ξ^-	183
K_L^0	15	**Si**	41	$\overline{\Xi}^0$	301

Table 1. Types and codes of nuclei and particles used in simulations and recording.

4 Materials

Table 2 lists the substances which can be used in simulation and their features. The last column displays notations used in *.DAT files. Points mean blank positions.

Substance	Radiation length, g/cm^2	Density g/cm^3	Notation
Polyethylene	44.64	0.95	`polyet`
Carbon	42.7	2.2	`carbon`
Stainless	13.84	7.87	`stainl`
Lead	6.37	11.35	`..lead`
glance paper	26.1	0.871	`gpaper`
Em-H	20.1	1.85	`..Em-H`
Em-M	22.7	1.70	`..Em-M`
HR-4	11.4	2.91	`..HR-4`
HR-8	12.2	2.54	`..HR-8`
X200	20.1	1.97	`..X200`
Lucite	40.49	1.20	`lucite`
Styrol	41.7	0.02	`styrol`
Rubber	42.2	1.15	`rubber`
Air	36.66	$1.205{\cdot}10^{-3}$	`...air`
H_2	61.28	1.0	`hydrog`
LiH	79.045	0.6	`...LiH`
Be	65.19	1.848	`....Be`

Table 2. Substances used in simulations and their features. The last column displays notations in simulations. Points in the last column mean blank positions.

5 Nuclear cascade

Interactions of nuclei and hadrons are simulated with the use of the MC0 code (Fedorova and Mukhamedshin, 1994). This code is based on quark-gluon string model (QGSM) (Shabelsky, 1988), semihard jet theory (Gribov *et al.*, 1983) and takes into account the generation of a large number of hadrons including strange and charmed mesons and baryons.

6 Electromagnetic cascade

Three-dimensional electromagnetic cascade in media is simulated with taking into account
- pair creation by $\gamma-$rays
- bremstrahlung radiation by electrons and positrons
- multiple Coulomb scattering
- ionization losses
- Compton scattering
- inelastic photonuclear interactions of $\gamma-$rays
- giant resonance absorption of low-energy $\gamma-$rays
- photo effect of low-energy $\gamma-$rays

The Landau-Pomeranchuk-Migdal effect is taken into account in pair production and bremsstrahlung processes at high energies. The differential and total cross sections of the LPM effect from (Galkin *et al*., 2000) calculated at a threshold of 100 keV are used.

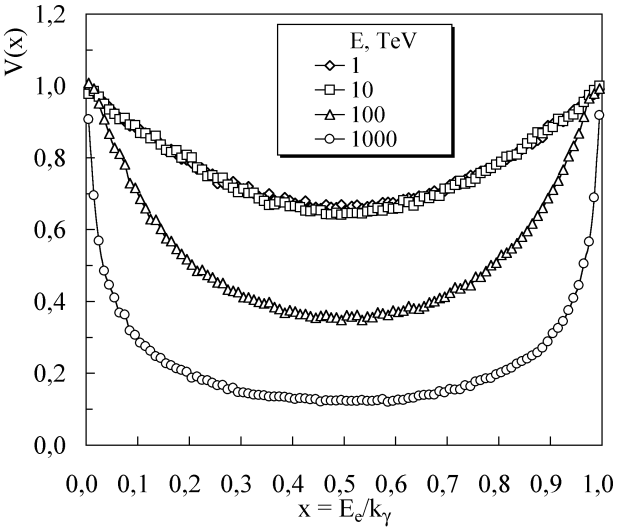

Fig. 1. Differential cross sections over $x = E_e/k_\gamma$ - fraction of energy transferred to electron in pair creation process in lead at various energies with taking into account the LPM effect realized by the *SPHINX*.

6.1 Pair creation

Fig. 1 demonstrates differential cross sections over electron-to-photon energy ratio $x = E_e/k_\gamma^0$ (fraction of energy transferred to electron in pair production process) in lead at various energies with taking into account the LPM effect realized by the *SPHINX*.

6.2 Bremsstrahlung

Fig. 2 demonstrates differential cross sections over photon-to-electron energy ratio $x = k_\gamma/E_e^0$ (fraction of energy transferred to γ in bremsstrahlung process) in lead at various energies with taking into account the LPM effect realized by SPHINX.

6.3 Compton scattering

The Compton scattering is sampled by using the differential cross section of energy ΔE transferred by $\gamma-$ray to electron

$$\frac{d\sigma_c}{d(\Delta E)} = \frac{3\Phi_0}{8qh\nu_0}\left[2 + \frac{\eta^2}{1-\eta} - \frac{\eta}{q^2}\frac{2q-\eta(1+2q)}{(1-\eta)^2}\right], \quad (1)$$

$$\text{where } \eta = \frac{\Delta E}{k_\gamma};\ \Phi_0 = \frac{8\pi}{3}\left(\frac{e^2}{mc^2}\right)^2,\ \Delta E = \frac{1}{k_\gamma} - \frac{1}{k_\gamma^0}, \quad (2)$$

k_γ^0 and k_γ are energies of $\gamma-$ray before and after Compton scattering, respectively.

6.4 Post-splitting scattering

It is taken into account that particles suffer the additional scattering characterized by the angle θ with respect to direction of the parent particle after the bremsstrahlung, pair

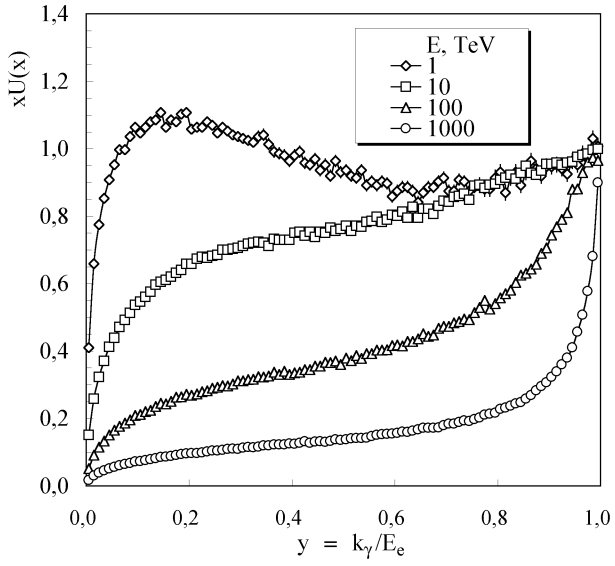

Fig. 2. Differential cross sections over fraction of energy transferred to γ, $x = k_\gamma/E_e$, in bremsstrahlung process in lead at various energies with taking into account the LPM effect realized by the *SPHINX*.

production, and Compton scattering. For bremsstrahlung and pair production, these angles are characterized by $\langle\theta^2\rangle^{1/2} = g(v)\ln p/p$ and $f(u)\ln q/q$, where $p = k_\gamma^0/m_e$, $v = E_e/k_\gamma^0$; $q = E_e^0/m_e$, $u = k_\gamma/E_e^0$. $f(u) \sim g(v) \simeq 1 \div 4$; $f(u)$ and $g(v)$ rather weakly depend on energy. Real angles are sampled by Gaussian distribution with accounting for energy of particles with the zero average value and the standard deviation $\sigma = \langle\theta^2\rangle^{1/2}$. In opposite to the case of pair production and bremsstrahlung, the kinematics of Compton scattering is unambiguous and angles of particles with respect to direction of initial $\gamma-$ray are easily calculated.

7 Computation of darkness

The *SPHINX* makes possible to simulate measurements of darkness of spots on X-ray films with using both the square slits (applied by RUNJOB, e.g.) and circle diaphragms (applied by the Pamir Collaboration, e.g.). In both the cases, to simulate the measurement process the area of the slit of L size (or diameter) is divided into K elementary square cells of l size.

Usually, the darkness of an area on X-ray film spot is calculated by RUNJOB and Pamir Collaborations with relations

$$D = D_0\left(1 - \frac{1}{1+\alpha\rho}\right) \text{ and } D = D_0\left(1 - e^{-s\rho}\right), \qquad (3)$$

respectively. Here $s = 3.25 \pm 0.13\,\mu\text{m}^2$ is an effective cross section of emulsion grain, $\alpha = 5.5\,\mu\text{m}^2$ is a similar value, ρ is the density of charged particle per unity square.

By definition, $I_i = I_{0_i}10^{-D_i}$, where D_i is the darkness "measured" by *i*th elementary cell, I_{0_i} and I_i are the light intensity before and after passage of the cell. As all I_{0_i} are the same, the total darkness "measured" by the large slit divided into K elementary cells is

$$D_{tot} = \lg\frac{\sum\limits_{i=1}^{K} I_{0_i}}{\sum\limits_{i=1}^{K} I_i} = \lg K - \lg\sum_{i=1}^{K} 10^{-D_i(N_e)} \qquad (4)$$

To simplify simulations with a square slit, the cell size is chosen so that the ratio $N = L/l$ is an integer number. Obviously, $K = N^2$.

The simulation of circle diaphragm is a little more complicated problem because a number of elementary cells is intersected and divided by the circle boundary into two parts (inside and outside the circle) with areas of s_{in} and s_{out}, respectively. This problem can be solved in two ways. At first, one can calculate the real area of each intersected cell which makes a contribution into the measured light flow and calculate the corresponding particle density. The second way is to assume that such cell contributes into the total measured light flow with the probability $w_i = s_{in}/(s_{in} + s_{out})$. Obviously, both the ways are equivalent in average. It is the first way which is used by the *SPHINX*.

7.1 Darkness maximization

The experimental procedure of darkness measurement has a stage of darkness maximization by a measuring person. The *SPHINX* takes also this factor into account by slit (diaphragm) scanning and measuring darkness values in a vicinity of the spot and selecting the maximum value among all the values "measured" during the scanning.

8 Testing

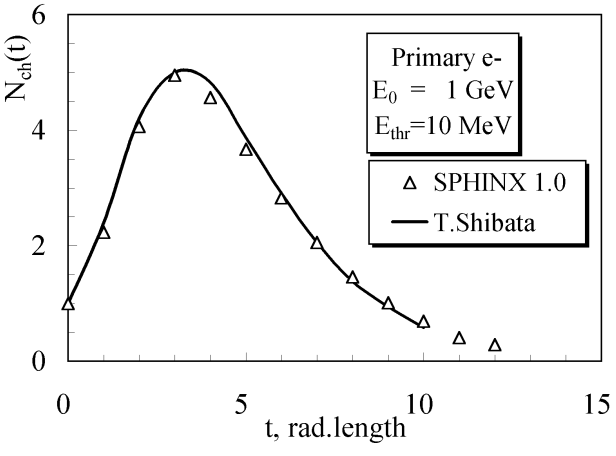

Fig. 3. Transition curves of electron-initiated cascades in lead at $E_e = 1$ GeV and $E_{thr} = 10$ MeV. Results by Okamoto and Shibata (1987) are shown by curve.

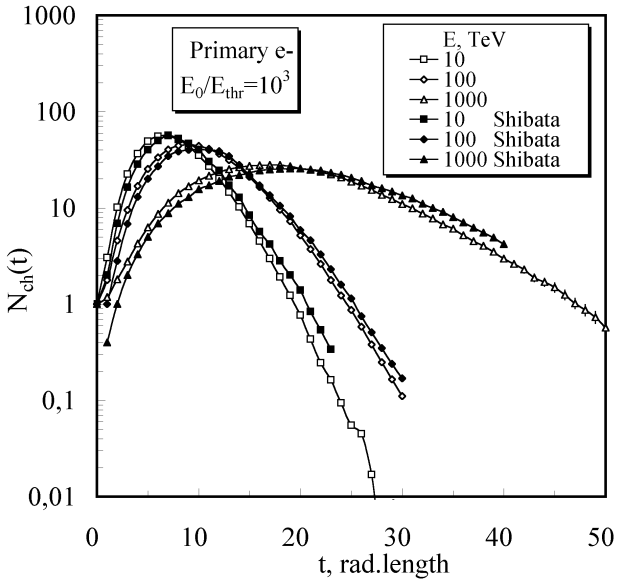

Fig. 4. Transition curves of electron-initiated cascades in lead at $E_e = 10, 100$ and 1000 TeV at $E_e/E_{thr} = 10^3$ at $E_e = 1$ GeV and $E_{thr} = 10$ MeV. Results by Okamoto and Shibata (1987) for γ-rays are also shown.

Fig. 3 demonstrates transition curves of electron-initiated cascades in lead at $E_e = 1$ GeV and $E_{thr} = 10$ MeV. Results by Okamoto and Shibata (1987) are also shown by curve.

Fig. 4 demonstrates transition curves of electron-initiated cascades in lead at $E_e = 10, 100$ and 1000 TeV at $E_e/E_{thr} = 10^3$. Results by Okamoto and Shibata (1987) for γ-rays are also shown. One can see a rather good agreement.

9 The *SPHINX* potentialities

The *SPHINX* code makes it possible
• to record information on first interaction of primary particle in the emulsion chamber;
• to record characteristics of secondary particles generated in the first interaction
• to select events in the emulsion chamber by darkness produced on X-ray films at fixed depths in the chamber;
• to record density of charged particles in elementary cells at fixed depths in the chamber
• to record darkness in elementary cells at fixed depths in the chamber.

10 Conclusion

The *SPHINX* code is elaborated for simulations of processes in X-ray emulsion chambers and measurement procedures used in experiments. The code is easy in use as well as it is easy of access for all the persons via Internet.

Acknowledgements. This work is supported by the RFBR, projects no. 00-15-96632 and 99-02-18173.

References

Dunaevsky,A.M. and Zimin, M.V., Proc. 5th ISVHECRI, Lodz (1988) 93
Fedorova, G.F. and Mukhamedshin, R.A. , Bull. Soc. Sci. Lettr. Lodz, Ser. Rech. Def. (1994), vol. XVI, 137
Galkin, V.I. *et al*., private communication
Gribov, L.V., Levin, E.M., and Ryskin, M.G. Phys.Reports 100, nos. 1,2, (1983), 1.
Haungs, A. *et al*., Nucl. Phys. B (Proc. Suppl.) 97 (2001) 131
Okamoto, M. and Shibata, T., Nuclear Instruments and Methods in Phys. Res. A257 (1987) 155
Shabelsky, Yu.M. Z.Phys.C, (1988) v.38, no. 4, 569